*Наносистеми, наноматеріали, нанотехнології*
*Nanosistemi, Nanomateriali, Nanotehnologii*
2026, т. 24, № 2, сс. 625–636
https://doi.org/10.15407/nnn.24.02.0625



PACS numbers: 61.46.Bc, 68.43.Bc, 68.43.Fg, 71.15.Mb, 73.20.Hb, 78.30.-j, 82.60.Qr

# Adsorption of Toxic Gases $CH_4$, $CO_2$ and $NH_3$ on Copper Nanoclusters

Lekshmi R Ganesh[1], V Baiju[2,6], Dedhila Devadathan[3,6], Abhilash S[4,6], and Y Sheena Mary[4,6]

[1]*SN College, Department of Physics, Varkala, India*
[2]*SN College, Department of Physics, Punalur, India*
[3]*SN College, Department of Physics, Kollam, India*
[4]*SN College, Department of Chemistry, Kollam, India*
[5]*FMN College, Department of Physics, Kollam, India*
[6]*University of Kerala, IN-695034 Thiruvananthapuram, India*

Designing a drug for the removal of a poisonous material is a great challenge. In order to design an efficient material, we have to optimise its molecular structure and study its various properties. Different methods are used to analyse the adsorption of analytes on molecules. It includes computational chemistry and related methods. In order to balance accuracy and computational expense, hybrid approaches like DFT are also used. This paper discusses the extensive details of the DFT application to the adsorption of Cu–Cu clusters. It is used to calculate the geometrical structures of $Cu_3$–$X$ ($X = CH_4$, $CO_2$, $NH_3$), which are based on Cu clusters, as well as their interactions and adsorption. This allows for the discussion, determination, and some calculations of their associated binding energies, adsorption energies, and other thermodynamic and electronic properties. The HOMO–LUMO (highest occupied molecular orbital (HOMO)–lowest unoccupied molecular orbital (LUMO)) and MEP (molecular electrostatic potential) evaluations of molecular-orbital electronic configurations are

also displayed. The positive and negative regions of the Cu clusters are designated by these structures. Surface-enhanced Raman spectroscopy (SERS) provides peak frequencies and intensities for the analytes/adsorbate and Cu–analytes ($CH_4$, $CO_2$, $NH_3$) clusters.

Розробка препарату для видалення отруйної речовини є великим викликом. Для розробки ефективного матеріялу ми маємо оптимізувати його молекулярну структуру та вивчити його різні властивості. Для аналізи адсорбції аналітів на молекулах використовуються різні методи. Це включає обчислювальну хемію та пов'язані з нею методи. Для балансування точности та обчислювальних витрат також використовуються гібридні підходи, такі як теорія функціонала густини (DFT). У цій статті обговорюються всебічно деталі застосування DFT щодо адсорбції кластерів Cu–Cu. DFT використовується для розрахунку геометричних структур $Cu_3$–$X$ ($X = CH_4$, $CO_2$, $NH_3$), які базуються на кластерах Cu, а також їхніх взаємодій та адсорбції. Це дає змогу обговорити, визначити та провести деякі розрахунки пов'язаних з ними енергій зв'язку, енергій адсорбції й інших термодинамічних та електронних властивостей. Також показано електронні конфіґурації молекулярних орбіталей, оцінені через HOMO–LUMO (найвищу зайняту молекулярну орбіталь (HOMO)–найнижчу незайняту молекулярну орбіталь (LUMO)) та MEP (молекулярний електростатичний потенціял). Позитивні та неґативні області кластерів Cu позначено цими структурами. Підсилена поверхнею Раманова спектроскопія (SERS) забезпечує частоти й інтенсивності піків для кластерів аналітів/адсорбатів та Cu–аналітів ($CH_4$, $CO_2$, $NH_3$).

**Key words:** adsorption clusters, adsorbate, density functional theory, nanoclusters.

**Ключові слова:** адсорбційні кластери, адсорбат, теорія функціоналу густини, нанокластери.

*(Received 21 December, 2024; in revised form, 28 August, 2025)*

## 1. INTRODUCTION

Reducing particle size, particularly, down to the atomic scale, can dramatically increase the specific active surface area, leading to enhanced performance in catalysis, electronic devices, sensors, and other applications [1–3].

The increased activity and effectiveness of downsized particles can be attributed to their high surface-to-volume ratio, surface geometric effects, unique electronic properties, and the influence of quantum size effects [4].

Gold, traditionally recognized as a noble metal due to its inertness in bulk form, exhibits remarkable catalytic properties, when reduced to nanoscale dimensions, particularly, at low temperatures.

Present work is focusing on copper and its clusters. When copper molecules combine with toxic gas molecules like $CH_4$, $CO_2$ and $NH_3$, they form adsorbate–metal complexes like $Cu_3CH_4$, $Cu_3CO_2$ and $Cu_3NH_3$ clusters. In this study, we discussed about the adsorption energies, chemical energies, changes in thermodynamic parameters, molecular electrostatic potential and Raman spectrum of copper and copper–toxic gas molecular complexes.

## 2. METHODS USED

Computational calculations are done using Gaussian 16 software package with density functional theory (DFT). DFT used a basis set of LANL2DZ for calculation. Raman spectrum of toxic gases and copper–toxic gas complexes were analyzed based on surface enhanced Raman scattering.

## 3. RESULTS AND DISCUSSION

### 3.1. Optimized Geometry

The interactions and adsorption properties of all specified geometries and Cu–$X$ ($X = CO_2$, $CH_4$, and $NH_3$) were calculated using DFT. The Gaussian 16 programme suite [5], which uses DFT and the CAMB3LYP/LANL2DZ functional, was used to compute structures in a vacuum. Figure 1 shows the optimized structures of $Cu_3$–$CH_4$, $Cu_3$–$CO_2$, and $Cu_3$–$NH_3$.

### 3.2. HOMO and LUMO

The distribution of HOMO and LUMO over atoms shows that π-bonds have been delocalized. The positive and negative hemispheres are represented in HOMO–LUMO by the red and green colours, respectively. In $Cu_3$, both the HOMO and LUMO are over the entire $Cu_3$. In the case of $Cu_3CH_4$, both HOMO and LUMO are over $Cu_3$; for

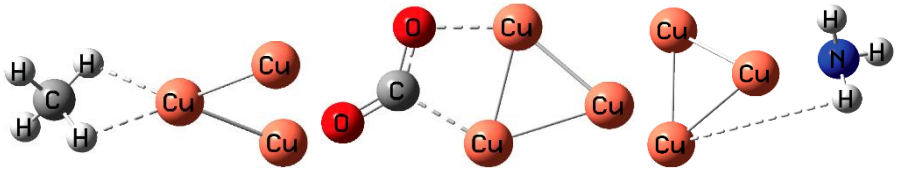


$Cu_3CH_4$ $Cu_3CO_2$ $Cu_3NH_3$

**Fig. 1.** The optimized structures of adsorbate–metal complexes.

$Cu_3CO_2$, both HOMO and LUMO are over the entire $Cu_3CO_2$, and for $Cu_3NH_3$, both HOMO and LUMO are over $Cu_3$.

### 3.3. Nonlinear Optical Properties

For the treatment of poisonous gases and vapours, which pass through porous substances like polymers and molecules, adsorption is a distinct and frequently employed approach [6]. Molecular-analyte complexes like $Cu_3$–$CH_4$, $Cu_3$–$CO_2$ and $Cu_3$–$NH_3$ are created, when copper atoms mix with molecules like $CH_4$, $CO_2$, and $NH_3$. In this section, the adsorption of copper metal clusters from the aforementioned copper complexes is assessed, using DFT method. The LANL2DZ functional is based on previous research with a similar structure, making it well suited for metal atoms [7]. The molecules $CH_4$, $CO_2$ and $NH_3$ are positioned close to metal clusters for optimisation, since they are in the most reactive positions. The adsorption energy is calculated by the equation $E_a = E_{Cu+X} - E_{Cu} - E_X$, where $E_{Cu+X}$—energies of the copper cluster with $X$ ($X = CH_4$, $CO_2$ or $NH_3$), $E_{Cu}$—energies of the copper cluster, $E_X$—energies of respective adsorbate ($CH_4$, $CO_2$ or $NH_3$).

Using Gaussian 16, we constructed the molecular structures of $Cu_3CH_4$, $Cu_3CO_2$ and $Cu_3NH_3$. In the ground state, $Cu_3$ clusters have a constant triangle shape [8]. The most stable form of $Cu_3$ is made up of four triangles with nine Cu–Cu bonds. The drug molecule is nearly planar, with the exception of the H atoms in $NH_3$. The H atom in $CH_4$, the O and C atoms in $CO_2$, and the N and H atoms in $NH_3$ are all potential sites for interaction with the $Cu_3$ cluster. The lone pairs in the $CH_4$, $CO_2$, and $NH_3$ unoccupied antibonding orbitals can accept electron density (ED) from the valence orbitals of metal atoms and supply the metal with electrons. The lone pair of electrons in $Cu_3$ clusters, which functions as proton acceptor, transmits charge to the H atom in $CH_4$, the O and C atoms in $CO_2$, and the N and H atoms in $NH_3$ [9]. In $Cu_3CH_4$, the distances are Cu–Cu = 2.32 Å, and $Cu_3$ is interacting with the H and C atoms of $CH_4$ with distances Cu–H = 2.07 Å and Cu–C = 2.45 Å. In $Cu_3CO_2$, the distances are Cu–Cu = 2.35 Å, and $Cu_3$ is interacting with the O and C atoms of $CO_2$ with distances Cu–C = 2.03 Å and Cu–O = 1.98 Å. In $Cu_3NH_3$, the distances are Cu–Cu = 2.35 Å, and $Cu_3$ is interacting with the H and N atoms of $NH_3$ with distances Cu–N = 2.00 Å and Cu–H = 2.52 Å. All the distances indicate an interaction between the toxic-gas molecules and $Cu_3$-nanocluster suggesting that the adsorption is chemisorptions.

The nonlinear optical (NLO) properties (Table 1) also exhibit changes in molecular systems: whereas the dipole moments of $CH_4$ and $CO_2$ are zero in complexes, the non-uniform charge density dis-

**TABLE 1.** Energy values, dipole moment, polarizability and adsorption energies of the molecules.

| System | Energy, Hartree | Dipole moment, D | Polarizability | Adsorption energy, kcal/mol |
|---|---|---|---|---|
| $CH_4$ | –40.514 | 0.00 | 11.70 | — |
| $CO_2$ | –188.54 | 0.0013 | 12.97 | — |
| $NH_3$ | –56.55 | 1.22 | 7.08 | — |
| $Cu_3$ | –592.07 | 0.57 | 125.25 | — |
| $Cu_3CH_4$ | –632.59 | 2.85 | 139.6 | –3.77 |
| $Cu_3CO_2$ | –780.64 | 5.24 | 105 | –18.83 |
| $Cu_3NH_3$ | –648.66 | 6.4 | 143.6 | –25.10 |

tribution, as demonstrated by the frontier molecular orbital (FMO) and molecular electrostatic potential (MEP) plots, causes an amplification of the dipole moment in complexes (Table 1). The $NH_3$ gas molecules' dipole moment varies as well. The polarizability of gas molecules increases after adsorption with $Cu_3$. The polarizabilities are of 11.70, 12.97 and 7.08 (a.u.) for $CH_4$, $CO_2$ and $NH_3$, while, after adsorption with $Cu_3$, the values are of 139.6, 105 and 143.6 (a.u.), respectively; this shows that the polarizability of the cluster often increases upon absorption by $Cu_3$ and proves that systems with higher polarizability are more reactive because their electron cloud is more flexible, which can enhance adsorption and make the adsorbate more chemically active on the surface. Higher polarizability of the adsorbent or adsorbate can lead to stronger dispersion. In this case, $Cu_3$ shows higher activity towards $NH_3$ adsorbate.

A large change in the dipole moment suggests strong charge transfer or polarization effects between adsorbent and adsorbate often indicating chemisorption. From Table 1, the strong bonding occurs in $Cu_3NH_3$. The adsorption energies provide a direct measure of how strongly the adsorbate is bound to the adsorbent. As all energies are of above 0.5 eV, it shows a strong adsorption involving covalent bond between the adsorbate and adsorbent.

### 3.4. Calculation of Energy Gap, Hardness, Chemical Potential, and Electrophilicity Index

After adsorption the energy gaps are of 1.87, 2.9 and 1.80 eV for $CH_4$, $CO_2$ and $NH_3$ complexes with $Cu_3$, while, for pure $CH_4$, $CO_2$ and $NH_3$, the corresponding values are of 6.51, 9.10 and 3.54 eV (Table 2). The energy gaps in the complexes are substantially lower than that of pure molecules value.

$Cu_3$–$CH_4$, $Cu_3$–$CO_2$, and $Cu_3$–$NH_3$ complexes' thermodynamic sta-

**TABLE 2.** Chemical descriptors of adsorbate and adsorbate–metal complexes.

| System | $E_H$, eV | $E_L$, eV | Energy gap, eV | Hardness, eV | Chemical potential, eV | Electrophilicity index, eV | $\Delta E_g$ |
|---|---|---|---|---|---|---|---|
| $CH_4$ | –10.60 | –4.09 | 6.51 | 3.26 | –7.35 | 8.29 | |
| $CO_2$ | –9.51 | –0.41 | 9.10 | 4.55 | –4.96 | 2.70 | |
| $NH_3$ | –6.20 | –2.66 | 3.54 | 1.77 | –4.43 | 5.54 | |
| $Cu_3$ | –4.25 | –2.90 | 1.35 | 0.68 | –3.58 | 9.42 | |
| $Cu_3CH_4$ | –4.0 | –2.13 | 1.87 | 0.94 | –3.07 | 5.01 | 32.5% |
| $Cu_3CO_2$ | –5.8 | –2.9 | 2.90 | 1.45 | –4.35 | 6.53 | 11.5% |
| $Cu_3NH_3$ | –3.45 | –1.65 | 1.80 | 0.90 | –2.55 | 3.61 | 33.3% |

**TABLE 3.** Thermodynamic parameters of adsorbate and adsorbate–metal complexes.

| System | $E$, Hartree | $H$, Hartree | $G$, Hartree | $S$, cal/(mol·K) |
|---|---|---|---|---|
| $CH_4$ | –40.46 | –40.46 | –40.49 | 44.48 |
| $CO_2$ | –188.53 | –188.53 | –188.55 | 42.74 |
| $NH_3$ | –56.51 | –56.51 | –56.53 | 46.76 |
| $Cu_3$ | –592.06 | –592.06 | –592.09 | 77.98 |
| $Cu_3CH_4$ | –632.54 | –632.53 | –632.58 | 101.86 |
| $Cu_3CO_2$ | –780.62 | –780.61 | –780.66 | 95.30 |
| $Cu_3NH_3$ | –648.62 | –648.61 | –648.66 | 90.326 |

bility is predicted, using binding energies and fluctuations in Gibbs energy (Tables 1–3).

The energy gap ($E_g$) is calculated by taking difference of HOMO and LUMO energies as $E_g = E_H - E_L$, where $E_H$ and $E_L$ are the HOMO and LUMO energies, respectively. The hardness ($\eta$) is calculated by dividing energy gap by 2: $\eta = E_g/2$, where $E_g$ is the energy gap. Similarly, the chemical potential ($\mu$) is calculated by taking mean of HOMO and LUMO energies, $\mu = (E_H + E_L)/2$, where $E_H$ and $E_L$ are the HOMO and LUMO energies, respectively. The electrophilicity index ($\omega$) is given as $\omega = \mu^2/(2\eta)$, where $\mu$ is the chemical potential and $\eta$ is the hardness.

When the energy values are negative, the adsorption process is

exothermic [10]. As a result, in these conditions, $CH_4$, $CO_2$ and $NH_3$ function as a nucleophilic reagent with the goal of binding to positively charged sites [11].

### 3.5. Thermodynamic Parameters

The entropy changes for all systems under considerations are negative, and the changes in the thermodynamic properties of the molecules also show that the adsorption process is spontaneous (Table 3). To evaluate the binding activity, we analysed the energies of the frontier orbitals in the drug, metal, and the resulting complexes. One of the most crucial factors in determining the electronic structure and chemical reactivity are the frontier orbital energies. For instance, it is possible to access qualitatively the kinetic stability, chemical stability, and electrical conductivity of metal clusters [12].

The change in enthalpy ($\Delta H$), entropy ($\Delta S$), Gibbs energy ($\Delta G$) and energy ($\Delta E$) (Table 4) can be calculated, using the equations

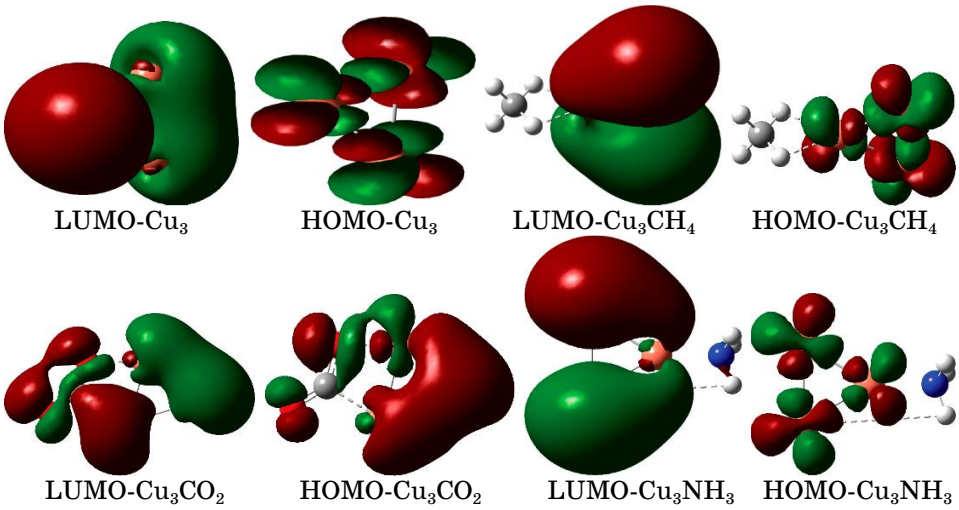


**Fig. 2.** HOMO–LUMO plots of adsorbate–metal complexes.

**TABLE 4.** Changes in thermodynamic parameters of adsorbate–metal complexes.

| System | $\Delta E$, kcal/mol | $\Delta H$, kcal/mol | $\Delta G$, kcal/mol | $\Delta S$, cal/(mol·K) |
|---|---|---|---|---|
| $Cu_3CH_4$ | –3.26 | –3.01 | –3.13 | –20.592 |
| $Cu_3CO_2$ | –17.44 | –17.81 | –10.23 | –25.414 |
| $Cu_3NH_3$ | –28.74 | –29.94 | –19.68 | –34.401 |

given below. The change in energy, $\Delta E$, is given as follows: $\Delta E = E_3 - E_2 - E_1$, where $E_3$, $E_2$ and $E_1$ are the energies of $Cu_3$–$X$ ($X = CH_4$, $CO_2$ and $NH_3$), $Cu_3$ and $X$ ($X = CH_4$, $CO_2$ and $NH_3$), respectively, in [kcal/mol]. Similarly, we can write the equations for change in entropy, enthalpy and Gibbs free energy as $\Delta H = H_3 - H_2 - H_1$, $\Delta G = G_3 - G_2 - G_1$, and $\Delta S = S_3 - S_2 - S_1$, where the terms have similar meanings.

The enthalpy change ($\Delta H$) gives direct insight into the strength of the interaction between the adsorbent and adsorbate. A negative $\Delta H$ value indicates that the complex formation is energetically favourable, meaning strong interactions between the adsorbent and adsorbate. All complexes with $Cu_3$ show negative values that proves $Cu_3$ as a very good adsorbent. Since all complexes have negative $\Delta G$ values, it indicates that the adsorption process is thermodynamically spontaneous.

### 3.6. Molecular Electrostatic Potential

The MEPs of both the cage and the gas molecules of adsorbed systems were also determined and interpreted. The blue area displays nucleophilic behaviour with insufficient electrons, while the red area illustrates electrophilic behaviour with sufficient electrons. Because of this, the blue region has a positive potential, whereas the red region has a negative potential, indicating that there will be a lot of positive charge binding in the blue region. C≡N, which is electrophilic, and hydrogen, which is nucleophilic, are the most active sites in all complexes. As a result, metal and gas molecules interact heavily.

In pure $Cu_3$, the third copper atom and two other copper atoms both exhibit a blue colour. $Cu_3CH_4$ has two Cu atoms, which are slightly yellow in colour, and one Cu atom that is blue. $CH_4$ also exhibits a blue colour. The three Cu atoms in $Cu_3CO_2$ are blue, while, in $CO_2$, the C and O atoms are somewhat blue and reddish

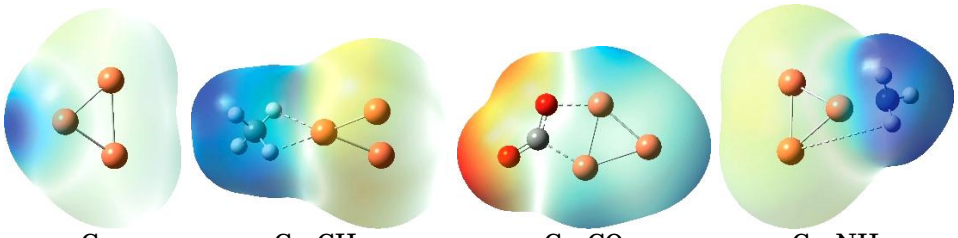


**Fig. 3.** Molecular electrostatic potential (MEP) maps for the adsorbate–metal complexes.

yellow, respectively. In $Cu_3NH_3$, the $NH_3$ group is positive and the one Cu atom close to it is somewhat blue. The other two Cu atoms apart from it are slightly yellow as seen in Fig. 3.

### 3.7. Intensity and Frequency of Analytes with Using Raman Spectrum

Figures 4, 5 and 6 show the Raman spectra of the analytes ($CH_4$, $CO_2$ and $NH_3$) and complexes. The frequency and intensity of these analytes and molecules were calculated, and the same were furnished in Table 5.

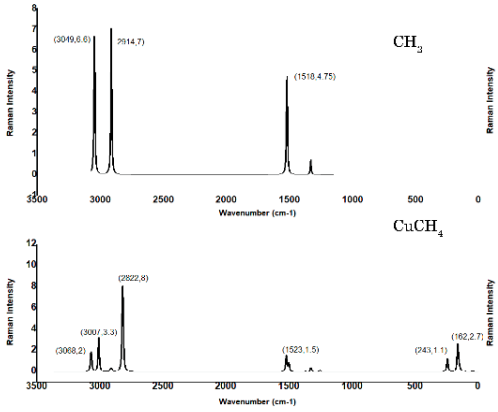


**Fig. 4.** Raman spectra of $CH_4$ molecule and the $CH_4$–nanocluster complexes.

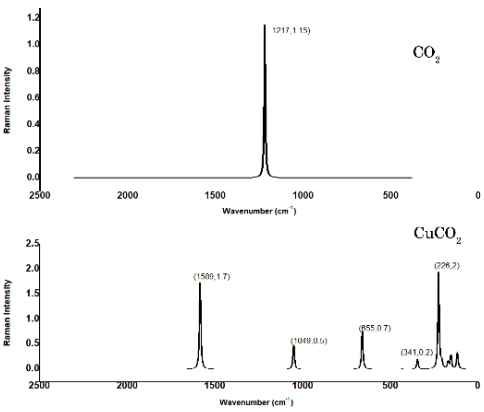


**Fig. 5.** Raman spectra of $CO_2$ molecule and the $CO_2$–nanocluster complexes.

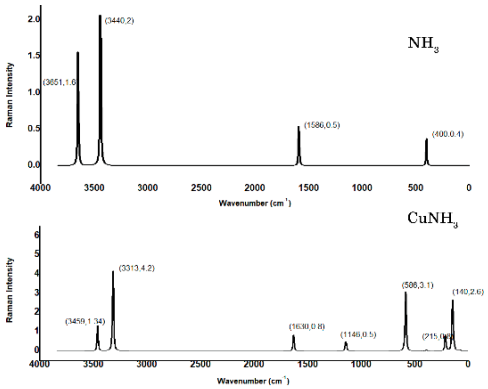


**Fig. 6.** Raman spectra of $NH_3$ molecule and the $NH_3$–nanocluster complexes.

**TABLE 5.** The frequency and intensity of the $CH_4$, $CO_2$ and $NH_3$ analytes and Cu–analyte molecules obtained with using Raman spectrum.

| System | Frequency | Intensity | Adsorption shift | Enhancement factor |
|---|---|---|---|---|
| $CH_4$ | 2914 | 7 | | |
| $CO_2$ | 1217 | 1.15 | | |
| $NH_3$ | 3440 | 2 | | |
| $Cu_3CH_4$ | 2822 | 8 | 3.16% | 14.3% |
| $Cu_3CO_2$ | 1589 | 1.7 | 30.57% | 47.83% |
| $Cu_3NH_3$ | 3313 | 4.2 | 3.7% | 110% |

Figure 4 shows the Raman spectra of $CH_4$ molecule and the $CH_4$–nanocluster complexes. In the $CH_4$ spectrum, stretching vibrations can be seen at wave number of 3000 $cm^{-1}$ and have an intensity of about 7. It has several peaks. $Cu_3CH_4$ has a peak at 3000 $cm^{-1}$ with an intensity of about 8. As shown in Fig. 5, $CO_2$ only has one band. The $CO_2$ spectrum can be seen at wave number of 1500 $cm^{-1}$ with higher peak intensity. $Cu_3CO_2$ demonstrates more than two bands. At wave number of 1500 $cm^{-1}$, a band with intensity of 1.5 was present. Stretching vibrations of the $NH_3$ molecule can be seen at wave numbers of 3500 $cm^{-1}$ and above with an intensity of 1.5, according to Fig. 6. $Cu_3NH_3$ exhibits a peak at wave number of 3500 $cm^{-1}$ with an intensity of about 4.

## 4. CONCLUSIONS

In this study, the application of DFT to the adsorption of Cu–Cu clusters provided a comprehensive analysis of the geometrical structures of $Cu_3$–$X$ clusters, where $X$ represents $CH_4$, $CO_2$, and $NH_3$. DFT calculations enabled the determination of the interactions and adsorption characteristics of these clusters, including their binding and adsorption energies, as well as other thermodynamic and electronic properties. From dipole-moment, polarizability and adsorption-energy studies, it is clearly shown that the interaction of $Cu_3$ with $CH_4$, $CO_2$, $NH_3$ are very strong, and it is chemisorption. From these studies, it also proves that $Cu_3$ shows higher activity towards $NH_3$ compared to $CO_2$ and $CH_4$. The study also presented the HOMO–LUMO analyses and MEP plots, which illustrated the positive and negative regions of the Cu clusters. The high negative HOMO energies of the $CH_4$, $CO_2$, and $NH_3$ adsorbate indicate poor nucleophilic behaviour. However, when these adsorbate form clusters with $Cu_3$, the resulting lower energy gap highlights the copper potential as an effective material for removing these toxic gases. The reactivity and stability of the cluster were studied, using

chemical potential, hardness and electrophilicity index; it was calculated by DFT. The calculation of entropy, enthalpy and free energy changes, using DFT, is crucial for understanding the thermodynamics of adsorbent and adsorbate interactions and predicting the feasibility of adsorbate-complex formation. Adsorbent materials for gas capture are evaluated based on how $\Delta H$, $\Delta S$, and $\Delta G$ change during adsorption. Lower $\Delta G$ values signify more effective adsorbents for capturing and storing gases; similarly, a negative $\Delta H$ value indicates that the complex formation is energetically favourable. Additionally, surface-enhanced Raman spectroscopy (SERS) data revealed the peak frequencies and intensities for both the analytes and Cu–analyte ($CH_4$, $CO_2$, $NH_3$) clusters. Raman studies (scattering phenomenon) of $Cu_3$–$X$ clusters are found to be a powerful tool for probing the adsorption mechanism behind the complexes.

## ACKNOWLEDGEMENTS

The authors express profound gratitude to Dr. Jamelah S. Al-Otaibi for her assistance in the computational studies.

## REFERENCES

1. Yuhang Li, Aoni Xu, Yanwei Lum, Xue Wang, Sung-Fu Hung, Bin Chen, Ziyun Wang, Yi Xu, Fengwang Li, Jehad Abed, Jianan Erick Huang, Armin Sedighian Rasouli, Joshua Wicks, Laxmi Kishore Sagar, Tao Peng, Alexander H. Ip, David Sinton, Hao Jiang, Chunzhong Li, and Edward H. Sargent, *Nat. Commun.*, **11**: Article No. 6190 (2020); https://doi.org/10.1038/s41467-020-20004-7
2. Takane Imaoka, Hirokazu Kitazawa, Wang-Jae Chun, and Kimihisa Yamamoto, *Angewandte Chemie Int. Ed.*, **54**, Iss. 34: 9810 (2015); https://doi.org/10.1002/anie.201504473
3. Tetsuya Kambe, Aiko Watanabe, Meijia Li, Takamasa Tsukamoto, Takane Imaoka, and Kimihisa Yamamoto, *Adv. Mater.*, **32**: 10 (2020), https://doi.org/10.1002/adma.201907167
4. Stephen U. S. Choi and Jeffrey A. Eastman, *Enhancing Thermal Conductivity of Fluids with Nanoparticles* (San Francisco, CA, United States: 1995).
5. Zakir Ullah, Aicha Kraimi, Hyun Jee Kim, Sooin Jang, Y. Sheena Mary, and Hyung Wook Kwon, *J. Molecular Liquids*, **359**: 119329 (2022); https://doi.org/10.1016/j.molliq.2022.119329
6. Deepu J. Babu, Divya Puthusseri, Frank G. Kühl, Sherif Okeil, Michael Bruns, Manfred Hampe, and Jörg J. Schneider, *J. Nanotechnol.*, **9**: 1782 (2018); https://doi.org/10.3762/bjnano.9.169
7. Sherin Joy, Vommina V Sureshbabu, and Ganga Periyasamy, *J. Phys. Chem. B*, **120**, Iss. 27: 6469 (2016); https://doi.org/10.1021/acs.jpcb.6b02210
8. Divya Maldepalli Govindachar and Ganga Periyasamy, *Chem. Phys. Lett.*, **753**: 137612 (2020); https://doi.org/10.1016/j.cplett.2020.137612

9. Pham Vu Nhat, Nguyen Thanh Si, Jerzy Leszczynski, and Minh Tho Nguyen, *Chem. Phys.*, **493**: 140 (2017); https://doi.org/10.1016/j.chemphys.2017.06.009
10. A. H. Pakiari and Z. Jamshidi, *J. Phys. Chem. A*, **111**, Iss. 20: 4391 (2007); https://doi.org/10.1021/jp070306t
11. Rahman Padash, Milad Rabbani Esfahani, and Ali Shokuhi Rad, *J. Biomol. Struct. Dyn.*, **39**, Iss. 15: 5427 (2021); https://doi.org/10.1080/07391102.2020.1792991
12. Jamelah S. Al-Otaibi, Y. Sheena Mary, Y. Shyma Mary, and Renjith Thomas, *Spectrochim. Acta*, **264**: 120233 (2022); https://doi.org/10.1016/j.saa.2021.120233
13. Ljubisa R. Radovic and Bradley Bockrath, *J. Am. Chem. Soc.*, **127**, Iss. 16: 5917 (2005); https://doi.org/10.1021/ja050124h